Five-fold differential cross sections for the ionization of aligned hydrogen molecule by electron and positron impact

R. Dey[a, *] , A. C. Roy[b], C. Dal Cappello[c]

[a] *Max-Planck-Institut für Plasmaphysik,*

Boltzmannstr. 2, D-85748 Garching, Germany

[b] *School of Mathematical Sciences, Ramakrishna Mission Vivekananda University,*

Belur Math 711202, West Bengal, India

[c] *Laboratoire de Physique Moleculaire et des Collisions,*

Institut de Physique, 1 Boulevard Arago, 57078 Cedex 3, France

Abstract

We report five-fold differential cross section (5DCS) for the ionization of aligned hydrogen molecule by electron and positron impact in coplanar geometry. The calculations have been performed for an incident energy of 200 eV and ejection energies of (3.5±2.5) and (16±4) eV. The present calculations are based on the eikonal approximation due to Glauber, and the BBK approximation. We have included the effect of post collision interaction (PCI) in the Glauber approximation classically. A comparison is made of the present calculations with the results of other theoretical methods and the recent experiment of Senftleben *et al.* [A. Senftleben, O. Al-Hagan, T. Pflüger, X. Ren, D. Madison, A. Dorn, J. Ullrich, J. Chem. Phys. 133 (2010) 044302]. The present theoretical models predict that the 5DCS is maximum when the intermolecular axis is aligned along the incident beam direction. The binary to recoil peak ratios predicted by the Glauber approximation with PCI (GA-PCI) are in reasonably good agreement with the experiment. The positions of the binary peaks predicted by the BBK approximation are also in good agreement with the experiment. The positron-impact ionization cross sections obtained in the BBK and GA-PCI methods are found to be higher than the electron-impact cross sections in the binary region while the converse is true for the recoil regime. In case of positron impact, the binary peaks predicted by both the GA-PCI and BBK models shifted away from the direction of momentum transfer, and showed a trend which is opposite to the case of electron impact ionization.

---

* Correspondence author. Tel:00498932991884
  E-mail address: ritud@ipp.mpg.de (R. Dey)

1. INTRODUCTION

Over the past two decades, the field of electron impact single ionization of one or two electron atomic target has reached a degree of maturity. Consequently, an increasing interest has grown in the study of ionization of more complex systems i.e. target as a molecule which is important for many fields such as radiation therapy, planetary atmospheres, near-stellar clouds and reactive plasmas. The fully differential cross section (FDCS) contains the complete information of an ionization process. Recently, attempts have been made both experimentally [1–4] and theoretically [3, 5–17] to get the FDCS for the ionization of simple diatomic hydrogen molecule by charged particle impact. In the case of diatomic molecules, the two-center geometry of the nuclear field can give rise to interference effects. Cohen and Fano [18] were the first to predict these effects long ago in the ionization of H_2 by photon impact. Subsequently, these interference effects were also predicted by Stia $et\ al.$ [19] for electron impact ionization of hydrogen molecule. But most of these attempts are devoted to non-aligned molecules. With the very recent experimental development of the fixed alignment of H_2 molecule [20–23] there has been a resurgence of theoretical study of FDCS using different models [24–27].

FDCS for the single ionization of an oriented dipolar molecule (5DCS) can be expressed as $\frac{d^5\sigma}{d\hat{\mathbf{k}}_1 d\hat{\mathbf{k}}_2 dE_2 d\phi_m d\theta_m}$, where $d\hat{\mathbf{k}}_1$ and $d\hat{\mathbf{k}}_2$ denote, respectively, elements of solid angles of the scattered projectile and the ejected electron, dE_2 represents the energy interval of the ejected electron and θ_m and ϕ_m fix the molecular alignment. Very recently, 5DCS for 200 eV electron impact ionization of hydrogen molecule has been explored experimentally as a function of molecular alignment by Senftleben $et\ al.$ [23, 28]. They derived the alignment of the internuclear axis from the fragmentation of the residual H_2^+ ion which was produced as a result of the ionizing collision. In fact, Senftleben $et\ al.$ [23, 28] considered the ground-state dissociation to study the alignment dependence of ionization into the electronic ground state of H_2^+. Moreover, they have compared their observations with the molecular three-body distorted wave model (M3DW) and the three Coulomb wave function approach. This three Coulomb wave function approach uses helium as a target wave function with an interference factor [19]. From now onwards, we will mention this approach as 3C-He approximation. In M3DW model, final-state Coulomb interaction between the projectile and screened nuclear charge, the Coulomb interaction between the ejected-electron and screened nuclear charge and the Coulomb interaction between projectile and ejected-electron are contained to all orders of perturbation theory. For the initial state of the above model the Coulomb interaction between the projectile and the screened nuclear charge for a neutral target is contained

to all orders of perturbation theory while the initial-state non spherical projectile-active-electron interaction is the first order interaction. Senftleben *et al.* [23, 28] have reported that M3DW reproduces most of the experimental results, although discrepancies remain. They have also mentioned that 3C-He failed to reproduce experimental FDCS at the ejection energy of (3.5±2.5) eV and the scattering angle of $(16\pm4)^o$.

In the present paper we have concentrated on the calculation of the 5DCS for the ionization of hydrogen molecule by electron and positron impact. We have compared the electron impact 5DCS with the M3DW [28] approximation, the 3C-He [23] approach and experimental data [23, 28]. In view of the recent demonstration of the feasibility of kinematically complete experiments for positron impact ionization of atoms using a reaction microscope [29], we have also studied 5DCS for aligned H_2 molecule. In this work we have applied the eikonal approximation due to Glauber (GA) [30] and the BBK approximation [31]. To the best of our knowledge the GA model is applied for the first time to calculate 5DCS using an interference factor. In the BBK amplitude, we have used atomic hydrogen wave function for the target and then multiply it with an interference factor given by Stia *et al.* [19] to obtain 5DCS. On the other hand, the Glauber approximation (GA) contains helium wave function as a target and the same interference factor. In the entrance channel, Glauber amplitude contains projectile-target correlation. In fact Glauber amplitude contains terms of all orders in V (i.e. the sum of the projectile-core and projectile-electron interactions) in its phase in an approximate way. In the exit channel we have introduced the post collision interaction (PCI) effect, i.e., projectile-ejected electron correlation in the GA (GA-PCI) following the semi-classical method used by Klar *et al.*[32]. On the other hand, BBK method uses an asymptotically exact scattering wave function which involves three appropriate confluent hypergeometric functions depending on the three pairwise inter-particle Coulomb interactions.

The GA has been successfully applied to a wide variety of atomic collisions [33–38]. Recently, Dey and Roy [38] applied the GA to study the role of projectile interactions in triply differential cross sections (TDCS) for excitation-ionization of helium and found that Glauber results are in reasonably good agreement with experiment for small scattering angles. The BBK method is also successfully applied to the various ionization processes [31, 39–41]. In 1989, Brauner *et al.* [31] have derived and applied the BBK model to calculate TDCS for ionization of hydrogen atoms by electrons and positrons and found excellent agreement with measurements at electron impact energies greater than 150 eV. Since then, the BBK wave function has been used by different authors to calculate fully and partly differential cross sections for the ionization of different target atoms by different charged particles and found to be reasonably successful to predict the measured data.

2. THEORY

The Glauber approximation has been described elsewhere [30, 42, 43], so only a brief outline will be presented here. The Glauber amplitude for the ionization of helium by an incident particle of charge z_P is given by (atomic units are used throughout, unless otherwise indicated) [35, 44]

$$F(\mathbf{q}, \mathbf{k_2}) = \frac{ik}{2\pi} \int d\mathbf{b} d\mathbf{r_1} d\mathbf{r_2} \phi_f^*(\mathbf{r_1}, \mathbf{r_2}) \Gamma(\mathbf{b}, \mathbf{r_1}, \mathbf{r_2}) \phi_i(\mathbf{r_1}, \mathbf{r_2}) \exp(i\mathbf{q}.\mathbf{b}), \tag{1}$$

where

$$\Gamma(\mathbf{b}, \mathbf{r_1}, \mathbf{r_2}) = 1 - \left(\frac{| \mathbf{b} - \mathbf{s_1} |}{b} \right)^{2i\eta} \left(\frac{| \mathbf{b} - \mathbf{s_2} |}{b} \right)^{2i\eta} \tag{2}$$

$\mathbf{q}=\mathbf{k}-\mathbf{k_1}$ and $\eta=-(\mu_P z_P/k)$. Here $\mathbf{k}$, $\mathbf{k_1}$ and $\mathbf{k_2}$ are the momenta of the incident particle, scattered projectile and ejected electron, respectively. μ_P represents the reduced mass of the system. $\mathbf{b}$, $\mathbf{s_1}$ and $\mathbf{s_2}$ are the respective projections of the position vectors of the incident particles and the two bound electrons onto the plane perpendicular to the direction of the Glauber path integration. In equation (1), $\mathbf{q}$, $\mathbf{b}$, $\mathbf{s_1}$ and $\mathbf{s_2}$ are coplanar. $\phi_i(\mathbf{r_1}, \mathbf{r_2})$ and $\phi_f(\mathbf{r_1}, \mathbf{r_2})$ represent the wave functions of the initial and the final states of the target, respectively. For the initial state of helium, we have chosen the analytical fit to the Hartree-Fock wavefunction given by Byron and Joachain [45]:

$$\phi_i(\mathbf{r_1}, \mathbf{r_2}) = U(\mathbf{r_1})U(\mathbf{r_2}) \tag{3}$$

where

$$U(\mathbf{r}) = (4\pi)^{-1/2}(Ae^{-ar} + Be^{-br})$$

$$A = 2.60505 \qquad B = 2.08144 \qquad a = 1.41 \qquad b = 2.61.$$

For the final-state target wave function we have used a symmetrised product of the He^+ ground state wavefunction for the bound electron times a Coulomb wave $\phi_{\mathbf{k_2}}$ orthogonalised to the ground state orbital

$$\phi_f(\mathbf{r_1}, \mathbf{r_2}) = 2^{-1/2}[\phi_{\mathbf{k_2}}(\mathbf{r_1})\nu(\mathbf{r_2}) + \nu(\mathbf{r_1})\phi_{\mathbf{k_2}}(\mathbf{r_2})], \tag{4}$$

where

$$\nu(\mathbf{r}) = (\lambda')^{3/2}\pi^{-1/2}e^{-\lambda'r}$$

$$\phi_{\mathbf{k_2}}(\mathbf{r}) = \chi_{\mathbf{k_2}}^{-}(\mathbf{r}) - \langle U(\mathbf{r}') \mid \chi_{\mathbf{k_2}}(\mathbf{r}')\rangle U(\mathbf{r})$$

$$\chi_{\mathbf{k_2}}^{-}(\mathbf{r}) = (2\pi)^{-3/2}exp(\frac{1}{2}\gamma\pi)\Gamma(1 + i\gamma)exp(i\mathbf{k_2}.\mathbf{r})_1F_1(-i\gamma, 1, -i(k_2r + \mathbf{k_2}.\mathbf{r}))$$

$$\gamma = 1/k_2 \qquad\qquad\qquad \lambda' = 2.$$

The triply differential cross section is given by

$$\frac{d^3\sigma}{d\hat{\mathbf{k}}_1 d\hat{\mathbf{k}}_2 dE_2} = \frac{k_1 k_2}{k} \mid F(\mathbf{q}, \mathbf{k_2}) \mid^2, \tag{5}$$

where $d\hat{\mathbf{k}}_1$ and $d\hat{\mathbf{k}}_2$ denote, respectively, elements of solid angles of the scattered projectile and the ejected electron and dE_2 represents the energy interval of the ejected electron. We have introduced the two-centre picture developed by Stia *et al.* [19] that predicts the interference effects. Hereby, 5DCS are obtained by multiplying TDCS with the interference factor

$$I = 2[1 + \cos((\mathbf{q} - \mathbf{k_2}).\mathbf{R})] \tag{6}$$

depending on the molecular alignment $\mathbf{R}$.

Popov and coworkers [46, 47] were the first to introduce a semiclassical method for the treatment of PCI in (e,2e) processes for an explanation of correct positions of binary and recoil peaks observed in triply differential cross sections. This method which described the shifts of paths of the outgoing electrons in (e,2e) experiments due to the coulomb interactions in the final state showed agreement with experiment. Later on, Popov and Erokhin [48] applied this method to (e$^+$, e$^+$e$^-$) process as a development of the (e,2e) method. Subsequently, Klar and coworkers [32, 49] extended this method to include both trajectory and energy shifts as follows:

$$\theta_i(0) = \theta_i - sin\delta \int_0^\infty dt\ r_1\ r_2\ r_{12}^{-3} \int_t^\infty dt'(r_i(t'))^{-2} \qquad i = 1, 2 \tag{7}$$

$$E_1(0) = E_1 + \frac{1}{r_1}|_{t=0} - \int_0^\infty dt\ \dot{r}_1\ r_{12}^{-3}(r_1 - r_2 cos\delta) \tag{8}$$

$$E_2(0) = E_2 - \int_0^\infty dt\ \dot{r}_2\ r_{12}^{-3}(r_2 - r_1 cos\delta) \tag{9}$$

5

where $\delta = \theta_1 + \theta_2$. $\theta_i(0)$ and $E_i(0)$ are the scattering angles and energies at the boundary of the short range region. The present GA calculation is performed using the same technique as was adopted by Roy *et al.* [43] that reduces the eight dimensional Glauber amplitude for the He(e,2e)He$^+$ process to a three dimensional integral.

In the BBK approximation, the triply differential cross section for the ionization of atomic hydrogen by an incident particle of charge z_P is given by,

$$\frac{d^3\sigma}{d\hat{\mathbf{k_1}}d\hat{\mathbf{k_2}}dE_2} = (2\pi)^4 \frac{k_1 k_2}{k} \mid T_{fi} \mid^2, \tag{10}$$

where the transition matrix element is

$$T_{fi} = \langle \Psi_f^- \mid V_i \mid \Phi_i \rangle. \tag{11}$$

In the above equation, the Φ_i and Ψ_f^- are the initial and final state wave function of the whole system, respectively. The initial state Φ_i is a product of an incoming plane wave and the ground state of hydrogen. V_i is the perturbation which contains projectile-target interaction. The final state wave function contains three appropriate confluent hypergeometric functions depending on three inter-particle Coulomb interactions.

$$\Psi_f^- = (2\pi)^{-3} exp(i\boldsymbol{k}_1.\boldsymbol{r}_1)exp(i\boldsymbol{k}_2.\boldsymbol{r}_2)C(\alpha_{PT}, \boldsymbol{k}_1, \boldsymbol{r}_1)C(\alpha_{eT}, \boldsymbol{k}_2, \boldsymbol{r}_2)C(\alpha_{eP}, \boldsymbol{k}_{12}, \boldsymbol{r}_{12}), \tag{12}$$

where the Coulomb part of the free-particle wavefunction is defined by

$$C(\alpha, \boldsymbol{k}, \boldsymbol{r}) = \Gamma(1 - i\alpha)exp(-\frac{1}{2}\pi\alpha)_1F_1(i\alpha; 1; -i(kr + \boldsymbol{k}.\boldsymbol{r}))$$

with

$$\alpha_{PT} = z_P z_T / k_1$$

$$\alpha_{eT} = -z_T / k_2$$

and

$$\alpha_{eP} = -\mu_P z_P / k_{12}$$

6

where, $\mathbf{k_{12}} = \frac{1}{2}(\mathbf{k_2}-\mathbf{k_1})$. Note that, in the initial state, we have used the hydrogen wave function with a variational charge 1.19 together with the corresponding normalisation factor is 0.5459. For the final state, z_T is replaced by $z_{eff}=\sqrt{-2\epsilon_i}$, ϵ_i =-0.566 a.u. the initial binding energy [50] and $z_P = -1$ or $+1$ for electron or positron impact, respectively. To obtain the 5DCS we have used the same interference factor as in Eq.(6).

3. RESULTS AND DISCUSSION

3.1. 5DCS for the molecules aligned relative to the incident beam direction

Figs.1-3 show the present 5DCS obtained in the BBK, GA and GA-PCI methods as a function of molecular alignment for the ionization of aligned hydrogen molecule by 200 eV electron impact at an ejection energy of E_2=(3.5±2.5) eV. The scattering angle is fixed at θ_1=(16±4)^o. The present geometry is coplanar. It means that the incident projectile, scattered projectile, ejected electron as well as the molecular axis all lie in the same plane. We observe that the magnitude of binary peak is largest when the molecule is aligned to the direction of the incident beam. In panels (a) and (b) of Fig.1 we present the BBK cross sections as a function of ξ which denotes the molecular alignment with respect to the incident beam direction. The binary maximum decreases with the increase of ξ, up to about 75° (see Table 1) and then starts rising till 90°. As a matter of fact the lowest value of the binary maximum is reached when the molecular alignment corresponds to the direction of momentum transfer. A similar trend is also noticed in Figs. 2 and 3 which contain GA and GA-PCI results, respectively for different values of ξ (see, also Table 1). In contrast to the plane wave first Born approximation (PWFBA) which uses a plane wave for the incoming projectile in the entrance channel, the GA uses a modified plane wave which includes in its phase projectile-target correlations. However, the exit channel in both the methods is described in exactly the same way. Furthermore, we notice that GA cross sections are greater than BBK results and differ by a considerable margin, although the overall distributions are nearly the same. With the increase of alignment angle BBK cross sections fall more steeply than the GA, while GA and GA-PCI 5DCS exhibit almost the same rate of fall. A comparison of GA and GA-PCI shows that the contribution of PCI is not appreciable and does not exceed 7% for the kinematics studied here. As there is no extensive experimental data for the above orientation it is not possible to assess the findings of the present theoretical predictions.

3.2. 5DCS for the molecules aligned relative to the direction of momentum transfer and comparison with the experiment

Figs. 4 and 5 show the comparisons of present GA, GA-PCI and BBK results with the M3DW, 3C-He and experimental data [23, 28] for 200 eV electron impact ionization of aligned hydrogen molecule at ejection energies of (3.5±2.5) and (16±4) eV, respectively, for coplanar geometry. The scattering angles are (5±2), (9.5±2.5) and (16±4)^o in panels (a), (b) and (c), respectively. The molecule is now aligned in the scattering plane at an angle (θ_m) of 90° relative to the direction of momentum transfer **q**. Senftleben *et al.* [28] have normalised the experimental data at the theoretical M3DW maximum for the θ_m=45° geometry. For sake of comparison, we have multiplied GA, GA-PCI, BBK, 3C-He and M3DW results by appropriate factors (see the scaling factors in the figure captions) to normalise them to the same point. It is worth noting that at low ejection energies of 3.5 eV the scaling factor in the M3DW differs from other theoretical models by a considerable factor of about 2 to 5. A similar observation has also been made by Ren *et al.* [4] that the perturbative M3DW model shows discrepancies concerning the absolute magnitude up to a factor of 6 in the (e,2e) study of H_2 at 16 eV above threshold. We notice that in the present kinematics PCI has a substantial contribution in both the binary and recoil regions and that GA-PCI results are better than the GA cross sections in comparison with the experimental data. We also observe that GA-PCI and BBK methods give similar distributions in the binary region as M3DW. However, in the recoil regime, the GA-PCI yields better distribution than the BBK. Nevertheless, a considerable discrepancy remains. One of the possible reason is that the present methods use an approximate formula for the interference factor. Fojón *et al.* [51] have calculated FDCS as a function of molecular alignment with respect to the momentum transfer direction at an incident energy of 4087 eV within the two-effective center approximation. They have pointed out that the indirect term and the symmetry of dissociative H_2^+ should be taken into account while using Stia's formula. However it is not easy to take into account of the above effects in our models. It will be possible if, for instance, we use a single-center wave function as in the reference "Second Born approximation for the ionization of H_2 by electron impact, Houamer *et al.*, J. Phys. B **36** (2003) 3009" but in this case it is not possible to apply the eikonal approximation or the BBK model. Second Born approximation (SBA) usually works very well for an incident energy of 200 eV and for an ejection energy of 3.5 eV. But the SBA calculations require a lot of computer time if we need high accuracy. As the present BBK and eikonal models have higher order contributions, they are expected to be effective in the intermediate energy region, say at 200 eV, at least for a

qualitative treatment.

Senftleben et al. [23] have also measured the 5DCS as a function of molecular alignment relative to the direction of momentum transfer and compared their results with the 3C-He calculations. They have found that 5DCS is maximum for molecules aligned along the direction of momentum transfer and it decreases with the increase of alignment angle in sharp contrast to the prediction of 3C-He method which shows an opposite behaviour. The present BBK and GA models also exhibit a similar behaviour as the 3C-He. The reason for this discrepancy may be ascribed to the approximate form of the interference factor proposed by Stia et al. [19]. It may be noted that Fojón et al. [51] have found that the magnitude of binary peak is not the largest when the molecules are aligned along the direction of momentum transfer. In fact, they have observed suppression of the binary peaks in the above case. Our results also confirm the findings of Fojón et al. [51] that the lowest value of binary maximum corresponds to the alignment of molecules along the momentum transfer. It is worth stressing that although the present models show discord in reproducing the observed experimental trend regarding the magnitudes of binary maxima as a function of alignment angles relative to the momentum transfer, nevertheless we notice in Table 2 that the binary peaks predicted by the present BBK theory are in good agreement with the M3DW model and experiment.

As the experimental data are relative we have calculated the ratio of binary to recoil peaks. Table 3 gives the summary of these ratios. A comparison with experiment shows that the ratios predicted by GA-PCI are better than those predicted by BBK theory for both the ejection energies, E_2=(3.5±2.5) and (16±4) eV and all scattering angles, θ_1=(5±2), (9.5±2.5) and (16±4)^o. The binary to recoil peak ratios predicted by the GA-PCI are also in better agreement with the measured peak ratios than the M3DW model for both the ejection energies (3.5±2.5) and (16±4) eV and scattering angles of (5±2) and (9.5±2.5)^o. The binary and recoil peaks predicted by the BBK and GA-PCI models are also in close agreement with the 3C-He model. However, the binary to recoil peak ratio predicted by the BBK approach differs considerably from 3C-He while GA-PCI is in reasonably good agreement with the ratio obtained in the 3C-He. Here we would like to mention that the difference between BBK and 3C-He calculations lies in the choice of the target wave function. For the BBK calculation it is the atomic hydrogen while 3C-He and GA-PCI involve the wave function of helium target. Furthermore, a comparison of present GA-PCI model with experiment shows that the introduction of PCI in the GA improves the binary to recoil peak ratio considerably.

Analogous to BBK and 3C calculations, we display in Figs. 6 and 7 the Glauber results obtained

9

in the GA-H and GA methods, respectively. The GA-H model uses atomic hydrogen as the target wave function while GA results are obtained with helium as the target wave function. The former model is based on the two-centre geometry of the nuclear field and calculates FDCS for the ionization of H_2 by multiplying the TDCS with the interference factor [19]. We observe that the binary peak positions predicted by GA-H, which involves the wave function of hydrogen target are in better accord with experiment than the GA calculation performed with the helium (see Table 4). But the binary to recoil peak ratio predicted by the GA are superior to GA-H everywhere in the present kinematics except at E_2=(3.5±2.5) eV and θ_1=(5±2)^o (also see Table 5).

Figs. 8 and 9 exhibit the present BBK (e$^+$) and GA-PCI (e$^+$) results for 200 eV positron impact along with the BBK (e$^-$), GA-PCI (e$^-$) and the experimental data for electron impact for ejection energies of (3.5±2.5) and (16±4) eV. The scattering angles are (5±2), (9.5±2.5) and (16±4)^o in panels (a), (b) and (c), respectively. The molecule is aligned in the scattering plane at an angle (θ_m) of 90° relative to the direction of momentum transfer **q**. The BBK (e$^+$) gives the higher binary maxima and lower recoil maxima than the corresponding BBK (e$^-$). Also the binary peak of BBK (e$^+$) shifted away from the direction of **q** in a opposite direction as in BBK (e$^-$). The reason is that there is a predominant attraction/repulsion between the projectile and the ejected electron in the final state when both of them move in the forward direction (binary peak). When the projectile and the ejected electron move in the opposite direction (recoil peak) the converse is true (see, Figs. 8 and 9). The positron impact GA-PCI (e$^+$) gives the similar results as the BBK (e$^+$) except at larger ejection energy and largest scattering angle. The PCI improves the GA results considerably in the case of electron impact. On the other hand, the binary peak of GA-PCI (e$^+$) is shifted in a direction opposite to that of GA-PCI (e$^-$) for all the ejection energies and for all scattering angles. This trend of shifting of binary peaks is consistent with the trend predicted in the semi-classical treatment of Popov and Erokhin [48]. The GA-PCI (e$^+$) cross sections are also higher than the corresponding GA-PCI (e$^-$) values. We notice that the positron and electron impact GA cross sections do not differ much throughout the distribution. This is because the GA lacks the post collision interaction effect in its amplitude.

Table 6 presents a comparison of angular positions of binary peaks as given by positron and electron impact 5DCS. A close inspection of these angular positions reveals that the difference between the peak positions for positron-impact BBK (e$^+$) and electron-impact BBK (e$^-$) decreases with the increase of scattering angles for both the ejection energies studied in the present kinematics. For example, at E_2=(3.5±2.5) eV the differences are 25, 19 and 8° for θ_1=(5±2), (9.5±2.5) and (16±4)^o, respectively. This is probably due to the post collision interaction effect which plays

10

an important role in the case of small scattering angles. The positions of the binary peaks of GA (e^+) are exactly the same as in the electron impact case. The reason is that GA cross sections are symmetric about the direction of momentum transfer $\mathbf{q}$. We also notice that there is a substantial difference between the angular positions of binary peak maximum for electron and positron impact GA-PCI results at E_2=(16±4) eV and θ_1=(16±4)^o while BBK gives the smallest difference (0°). It may be due to a completely different description of PCI factor in the GA-PCI model. However, in the absence of absolute data for positron impact 5DCS of aligned hydrogen molecule we are not able to make a critical study of different binary peaks predicted by different theoretical models considered in this work.

4. CONCLUSIONS

We have applied the GA, GA-PCI and BBK methods to calculate five-fold differential cross section for aligned hydrogen molecule by incorporating the interference factor due to Stia et $al.$ [19]. We have used the above methods for coplanar geometry for single ionization of H_2 molecule by electron and positron impact at an incident energy of 200 eV and for ejection energies of (3.5±2.5) and (16±4) eV and for scattering angles of (5±2), (9.5±2.5) and (16±4)^o. At E_2= (3.5±2.5) eV and θ_1=(16±4)^o we have studied the variation of 5DCS by electron impact with the different molecular alignments (ξ) relative to the incident beam direction. We find that the binary maxima predicted by the GA, GA-PCI and BBK methods decrease with the increase of ξ, up to about 75° and then start rising till 90°.

In the case of fixed molecular alignment of 90° with respect to the direction of momentum transfer $\mathbf{q}$, we have compared our results with the available experimental data and find that the binary peak positions obtained in the BBK model are superior to the corresponding GA-PCI results for both the ejection energies and most of the scattering angles. Since the experimental data are relative we have considered the ratios of binary/recoil peak and found that GA-PCI predictions are noticeably better than the M3DW calculation. We have also noticed that the introduction of PCI effect in the GA considerably improves the binary peak positions and binary to recoil peak ratios all over the kinematics studied in the present investigation. Both the binary and recoil peaks predicted by the BBK and GA-PCI models are also in close agreement with the 3C-He model, whereas in ratio comparison, BBK differs considerably from 3C-He while GA-PCI shows reasonably good agreement with 3C-He.

The GA-PCI and BBK also show that 5DCS differs substantially with the change of charge sign

of the projectile. Both the BBK (e^+) and GA-PCI (e^+) gives the higher binary maxima and lower recoil maxima than the corresponding BBK (e^-) and GA-PCI (e^-). Also the binary peak positions of BBK and GA-PCI results in case of positron impact shifted away from the direction of $\mathbf{q}$ in the opposite direction as in the electron impact case. It is noticed that the effect of postcollision interaction is maximum at E_2= (3.5±2.5) eV and θ_1=(5±2)^o i.e. for smallest ejection energy and smallest scattering angle. Absolute measurements of 5DCS for positron impact in the aforesaid energy region would be extremely valuable for testing the effectiveness of different theoretical models.

ACKNOWLEDGMENTS

[1] D. S. Milne-Brownlie, M. Foster, J. Gao, B. Lohmann, D. H. Madison, Phys. Rev. Lett. 96 (2006) 233201.

[2] E. M. Staicu Casagrande, A. Naja, F. Mezdari, A. Lahmam-Bennani, P. Bolognesi, B. Joulakian, O. Chuluunbaatar, O. Al-Hagan, D. H. Madison, D. V. Fursa, I. Bray, J. Phys. B 41 (2008) 025204.

[3] O. Al-Hagan, C. Kaiser, D. Madison, A. J. Murray, Nature Phys. 5 (2009) 59.

[4] X.Ren, A. Senftleben, T. Pflüger, A. Dorn, J. Colgan, M. S. Pindzola, O. Al-Hagan, D. H. Madison, I. Bray, D. V. Fursa, J. Ullrich, Phys. Rev. A 82 (2010) 032712.

[5] I. E. McCarthy, J. Phys. B 6 (1973) 2358.

[6] A.L. Monzani, L. E. Machado, M. T. Lee, A. M. Machado, Phys. Rev. A 60 (1999) R21.

[7] P. Weck, O. A. Fojón, J. Hanssen, B. Joulakian, R. D. Rivarola, Phys. Rev. A 63 (2001) 042709.

[8] P. F. Weck, A. Fojón, B. Joulakian, C. R. Stia, J. Hanssen, R. D. Rivarola, Phys. Rev. A 66 (2002) 012711.

[9] C. R. Stia, O. A. Fojón, P. F. Weck, J. Hanssen, B. Joulakian, R.D. Rivarola, Phys. Rev. A 66 (2002) 052709.

[10] J. Gao, J. L. Peacher, D. H. Madison, J. Chem. Phys. 123 (2005) 204302.

[11] V. V. Serov, B. B. Joulakian, V. L. Derbov, S. I. Vinitsky, J. Phys. B 38 (2005) 2765.

[12] J. Colgan, M.S. Pindzola, F. Robicheaux, C. Kaiser, A.J. Murray, D. H. Madison, Phys. Rev. Lett. 101 (2008) 233201.

[13] O. Chuluunbaatar, B. B. Joulakian, I. V. Puzynin, Kh. Tsookhuu, S. I. Vinitsky, J. Phys. B 41 (2008) 015204.

[14] E. M. Staicu Casagrande, A. Naja, A. Lahmam-Bennani, A. S. Kheifets, D. H. Madison, B. Joulakian,

J. Phys. : Conf. Series 141 (2008) 012016.

[15] V. V. Serov, B. B. Joulakian, Phys. Rev. A 80 (2009) 062713.

[16] J. Colgan, O. Al-Hagan, D. H. Madison, C. Kaiser, A. J. Murray, M. S. Pindzola, Phys. Rev. A 79 (2009) 052704.

[17] V. V. Serov, B. B. Joulakian, Phys. Rev. A 82 (2010) 022705.

[18] H. D. Cohen, U. Fano, Phys. Rev. 150 (1966) 30.

[19] C. R. Stia, O. A. Fojón, P. F. Weck, J. Hanssen, R. D. Rivarola, J. Phys. B 36 (2003) L257.

[20] M. Takahashi, N. Watanabe, Y. Khajuria, K. Nakayama, Y. Udagawa, J. H. D. Eland, J. Electron. Spectrosc. Realt. Phenom. 141 (2004) 83.

[21] M. Takahashi, N. Watanabe, Y. Khajuria, Y. Udagawa, J. H. D. Eland, Phys. Rev. Lett. 94 (2005) 213202.

[22] S. Bellm, J. Lower, E. Weigold, D. W. Mueller, Phys. Rev. Lett. 104 (2010) 023202.

[23] A. Senftleben, T. Pflüger, X. Ren, O. Al-Hagan, B. Najjari, D. Madison, A. Dorn, J. Ullrich, J. Phys. B 43 (2010) 081002.

[24] J. Gao, D. H. Madison, J. L. Peacher, J. Phys. B 39 (2006) 1275.

[25] M. S. Pindzola, F. Robicheaux, S. D. Loch, J. C. Berengut, T. Topcu, J. Colgan, M. Foster, D. C. Griffin, C. P. Ballance, D. R. Schultz, T. Minami, N. R. Badnell, M. C. Witthoeft, D. R. Plante, D. M. Mitnik, J. A. Ludlow, U. Kleiman, J. Phys. B 40 (2007) R39.

[26] J. Colgan, O. Al-Hagan, D. H. Madison, A. J. Murray, M. S. Pindzola, J. Phys. B 42 (2009) 171001.

[27] D. H. Madison, O. Al-Hagan, J. At. Mol. Phys. 2010 (2010) 367180.

[28] A. Senftleben, O. Al-Hagan, T. Pflüger, X. Ren, D. Madison, A. Dorn, J. Ullrich, J. Chem. Phys. 133 (2010) 044302.

[29] T. Pflüger, M. Holzwarth, A. Senftleben, X. Ren, A. Dorn, J. Ullrich, L. R. Hargreaves, B. Lohmann, D. S. Slaughter, J. P. Sullivan, J. C. Lower, S. J. Buckman, J. Phys. : Conf. Series 262 (2011) 012047.

[30] R. J. Glauber, in: W. E. Brittin, et al (Eds), Lectures in the Theoretical Physics, Vol. I, Interscience New Work, (1959) p.315.

[31] M. Brauner, J. S. Briggs, H. Klar, J. Phys. B 22 (1989) 2265.

[32] H. Klar, A. C. Roy, P. Schlemmer, K. Jung, H Ehrhardt, J. Phys. B 20 (1987) 821.

[33] R. Dey, A. C. Roy, Phys. Lett. A 332 (2004) 60 .

[34] R. Dey, A. C. Roy, Phys. Lett. A 353 (2006) 341.

[35] R. Dey, A. C. Roy , C. Dal Cappello, Nucl. Instrum. Methods B 266 (2008) 242.

[36] R. Dey, A. C. Roy, Nucl. Instrum. Methods B 267 (2009) 2357.

[37] M. Schulz, A. C. Laforge, K. N. Egodapitiya, J. S. Alexander, A. Hasan, M. F. Ciappina, A. C. Roy, R. Dey, A. Samolov, A. L. Godunov, Phys. Rev. A 81 (2010) 052705.

[38] R. Dey, A. C. Roy, Nucl. Instrum. Methods B 269 (2011) 364.

[39] M. Brauner, J. S. Briggs, H. Klar, J. T. Broad, T. Rösel, K. Jung, H. Ehrhardt, J. Phys. B 24 (1991) 657.

[40] S. Jones, D. H. Madison, Phys. Rev. A 65 (2002) 052727.

[41] C. Dal Cappello, A.C. Roy, X.G. Ren, R. Dey, Nucl. Instrum. Methods B 266 (2008) 570.

[42] A. C. Roy, A. K. Das, N. C. Sil, Phys. Rev. A 23 (1981) 1662.

[43] A. C. Roy, A. K. Das, N. C. Sil, Phys. Rev. A 28 (1983) 181.

[44] A. Igarashi, N. Toshima, T. Ishihara, Phys. Rev. A 45 (1992) R6157.

[45] F. W. Byron Jr, C. J. Joachain, Phys. Rev. 146 (1966) 1.

[46] Yu. V. Popov, J.J. Benayoun, J. Phys. B 14 (1981) 3513.

[47] Yu. V. Popov, J. Bang, J.J. Benayoun, J. Phys. B 14 (1981) 4637.

[48] Yu. V. Popov, V. F. Erokhin, Phys. Lett. A 97 (1983) 280.

[49] H. Klar, A. Franz, H. Tenhagen, Z. Phys. D 1 (1986) 373.

[50] C. Dimopoulou, R. Moshammer, D. Fischer, C. Höhr, A. Dorn, P. D. Fainstein, J. R. Crespo López Urrutia, C. D. Schröter, H. Kollmus, R. Mann, S. Hagmann, J. Ullrich, Phys. Rev. Lett. 93 (2004) 123203.

[51] A. Fojón, C. R. Stia, R. D. Rivarola, J. Phys. : Conf. Series 288 (2011) 012005.

Fig. 1: Coplanar five-fold differential cross section for single ionization of aligned hydrogen molecule by 200 eV electron impact as a function of the ejected electron angle for a fixed value of ejected electron energy E_2=(3.5±2.5) eV. The scattering angle is fixed at (16±4)^o. In panel (a), the curve with crosses represents the present BBK calculation for molecules aligned in the scattering plane at an angle ξ=0° with respect to beam direction. The dashed-dot curve represents the BBK result with ξ=15°. The solid curve represents the BBK result with ξ=30°. The dotted curve represents the BBK result with ξ=45°. In panel (b), the dashed curve represents the BBK result with ξ=60°. The solid curve represents the BBK result with ξ=75°. The dotted curve represents the BBK result with ξ=90°.

Fig. 2: As in Fig.1 except that the curves now represent the GA results.

Fig. 3: As in Fig.1 except that the curves now represent the GA-PCI results.

Fig. 4: Coplanar five-fold differential cross section for the single ionization of aligned hydrogen molecule by 200 eV electron impact as a function of the ejected electron angle. The molecule is aligned in the scattering plane at an angle of 90° relative to the direction of momentum transfer **q**. The ejected electron energy is (3.5±2.5) eV while the scattering angles are (a) (5±2)^o, (b) (9.5±2.5)^o and (c) (16±4)^o. In each panel, the solid curve represents the present GA-PCI results. The dashed-dot curve represents the present GA results. The dashed curve represents the present BBK results. The solid curve with cross represents the M3DW results [28]. The open circles with error bars are the experimental data [23, 28]. In panel(c), the dotted curve represents the 3C-He results [23]. The GA-PCI, GA, BBK and M3DW results are multiplied by 0.24, 0.18, 0.32 and 1.05, respectively in (a). The GA-PCI, GA and BBK results are multiplied by 0.265, 0.235 and 0.34, respectively in (b). The GA-PCI, GA, BBK, M3DW and 3C-He results are multiplied by 0.36, 0.36, 0.55, 0.88 and 0.40, respectively in (c).

Fig. 5: Same as Fig. 4, but at an ejected electron energy of (16±4) eV. The GA-PCI, GA, BBK and M3DW results are multiplied by 0.23, 0.155, 0.63 and 1.04, respectively in (a). The GA-PCI, GA, BBK and M3DW results are multiplied by 0.40, 0.31, 0.74 and 1.02, respectively in (b). The GA-PCI, GA, BBK and M3DW results are multiplied by 0.75, 0.67, 0.75 and 0.97,

respectively in (c).

Fig. 6: Coplanar five-fold differential cross section for the single ionization of aligned hydrogen molecule by 200 eV electron impact as a function of the ejected electron angle. The molecule is aligned in the scattering plane at an angle of 90° relative to the direction of momentum transfer $\mathbf{q}$. The ejected electron energy is (3.5 ± 2.5) eV while the scattering angles are (a) (5 ± 2), (b) (9.5 ± 2.5) and (c) $(16\pm4)^o$. In each panel, the solid curve represents the present GA-H results. The dashed curve represents the present GA results. The open circles with error bars are the experimental data [23, 28]. The GA-H and GA results are multiplied by 0.34 and 0.18, respectively in (a). The GA-H and GA results are multiplied by 0.26 and 0.235, respectively in (b). The GA-H and GA results are multiplied by 0.59 and 0.36, respectively in (c).

Fig. 7: Same as Fig. 6, but at an ejected electron energy of (16 ± 4) eV. The GA-H and GA results are multiplied by 0.28 and 0.155, respectively in (a). The GA-H and GA results are multiplied by 0.53 and 0.31, respectively in (b). The GA-H and GA results are multiplied by 0.88 and 0.67, respectively in (c).

Fig. 8: Coplanar five-fold differential cross section for the single ionization of aligned hydrogen molecule by 200 eV positron impact as a function of the ejected electron angle. The molecule is aligned in the scattering plane at an angle of 90° relative to the direction of momentum transfer $\mathbf{q}$. The ejected electron energy is (3.5 ± 2.5) eV while the scattering angles are (a) $(5\pm2)^o$, (b) $(9.5\pm2.5)^o$ and (c) $(16\pm4)^o$. In each panel, the solid curve represents the present BBK (e^+) results for positron impact. The dashed curve represents the present BBK (e$^-$) results for electron impact. The dotted curve represents the present GA-PCI (e^+) results. The dashed-dot curve represents the present GA-PCI (e$^-$) results. The open circles with error bars are the experimental data [23, 28] for electron impact. The BBK (e^+), BBK (e$^-$),GA-PCI (e^+) and GA-PCI (e$^-$) results are multiplied by 0.095, 0.32,0.225 and 0.24, respectively in (a). The BBK (e^+), BBK (e$^-$),GA-PCI (e^+) and GA-PCI (e$^-$) results are multiplied by 0.165, 0.34, 0.24 and 0.265, respectively in (b). The BBK (e^+), BBK (e$^-$), GA-PCI (e^+) and GA-PCI (e$^-$) results are multiplied by 0.35,0.55, 0.325 and 0.36, respectively in (c).

Fig. 9: Same as Fig. 8, but at an ejected electron energy of (16 ± 4) eV. The BBK (e$^+$), BBK (e$^-$), GA-PCI (e^+) and GA-PCI (e$^-$) results are multiplied by 0.14, 0.63, 0.17 and 0.23,

respectively in (a). The BBK (e^+), BBK (e^-), GA-PCI (e^+) and GA-PCI (e^-) results are multiplied by 0.33, 0.74, 0.31 and 0.40, respectively in (b). The BBK (e^+), BBK (e^-), GA-PCI (e^+) and GA-PCI (e^-) results are multiplied by 0.57, 0.75, 0.56 and 0.75, respectively in (c).

Table Captions:

Table 1: Binary peak maximum for different molecular alignments, as given by different theories.

Table 2: Comparison of binary and recoil peak positions.

Table 3: Comparison of binary and recoil peak ratios.

Table 4: Comparison of binary and recoil peak positions.

Table 5: Comparison of binary and recoil peak ratios.

Table 6: Comparison of binary peak position for electron and positron impact, as given by different theories.
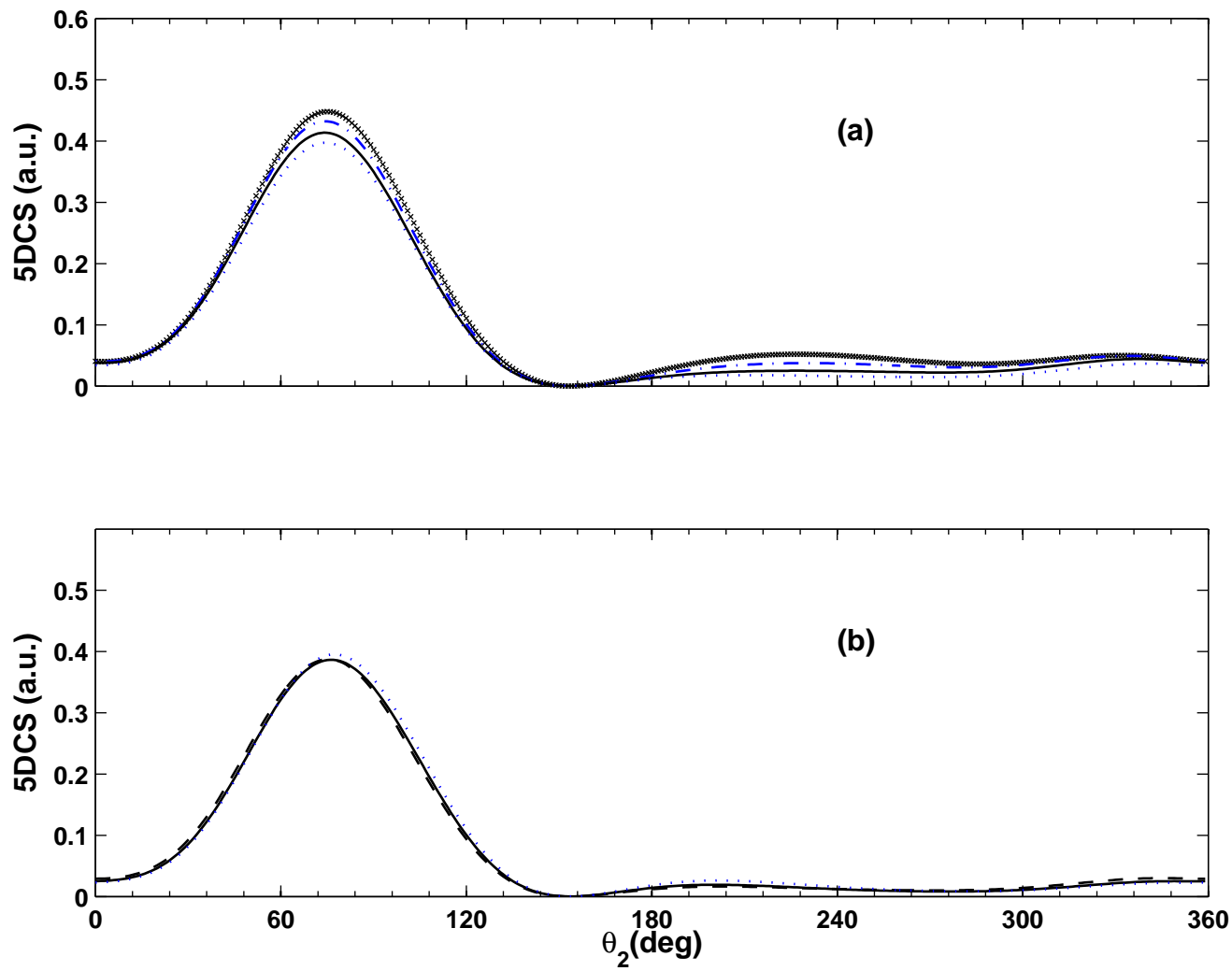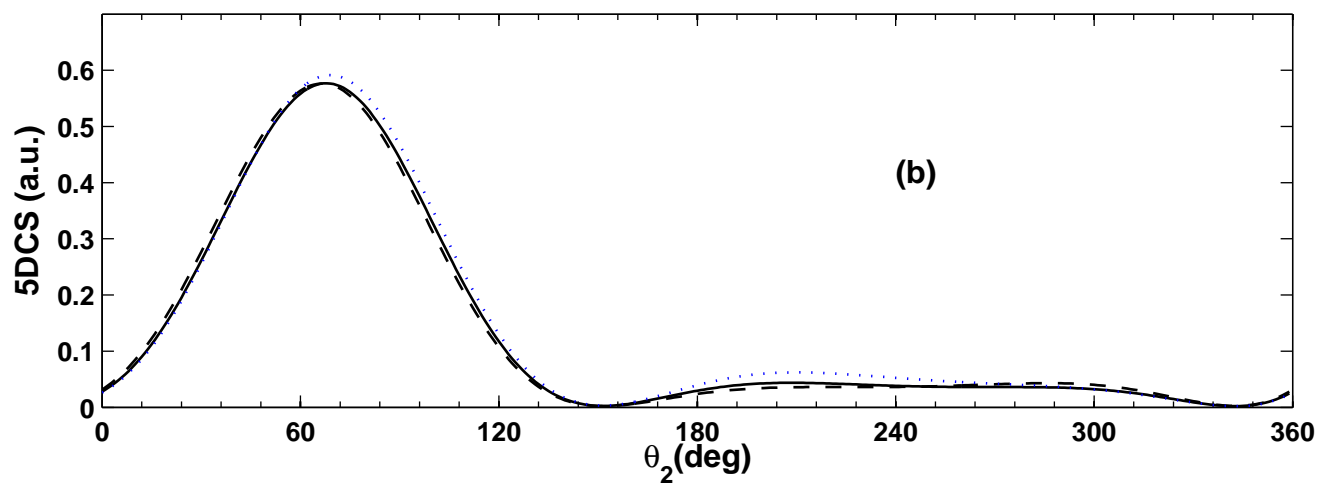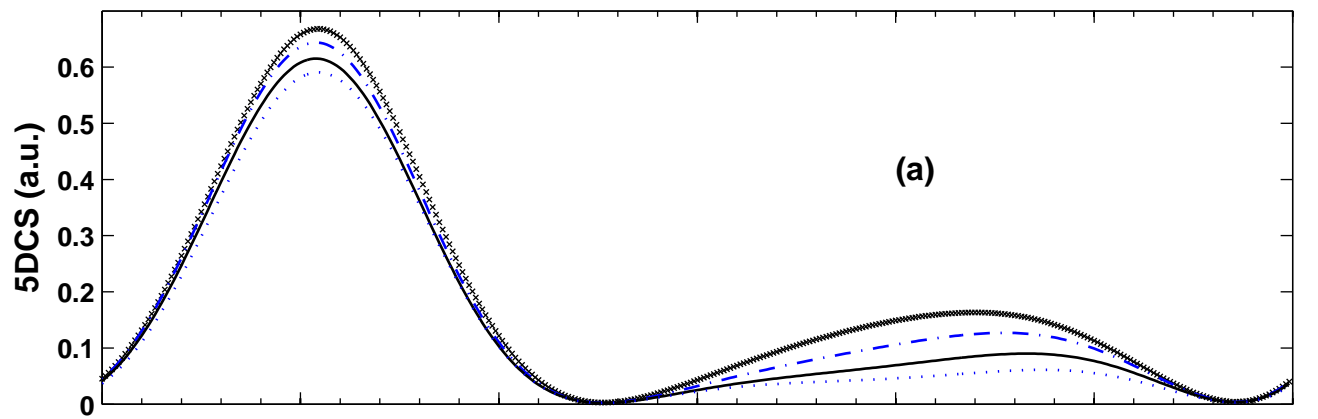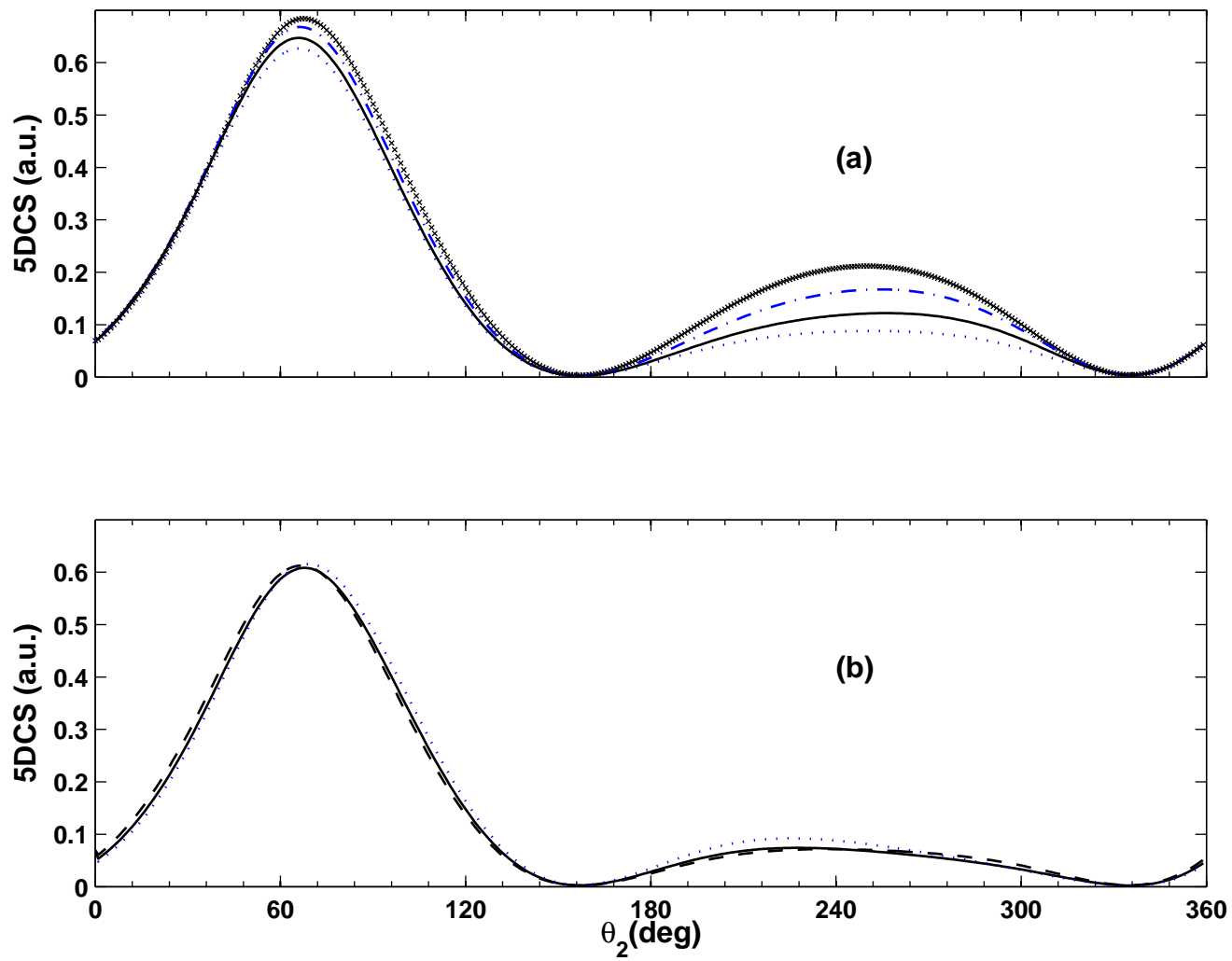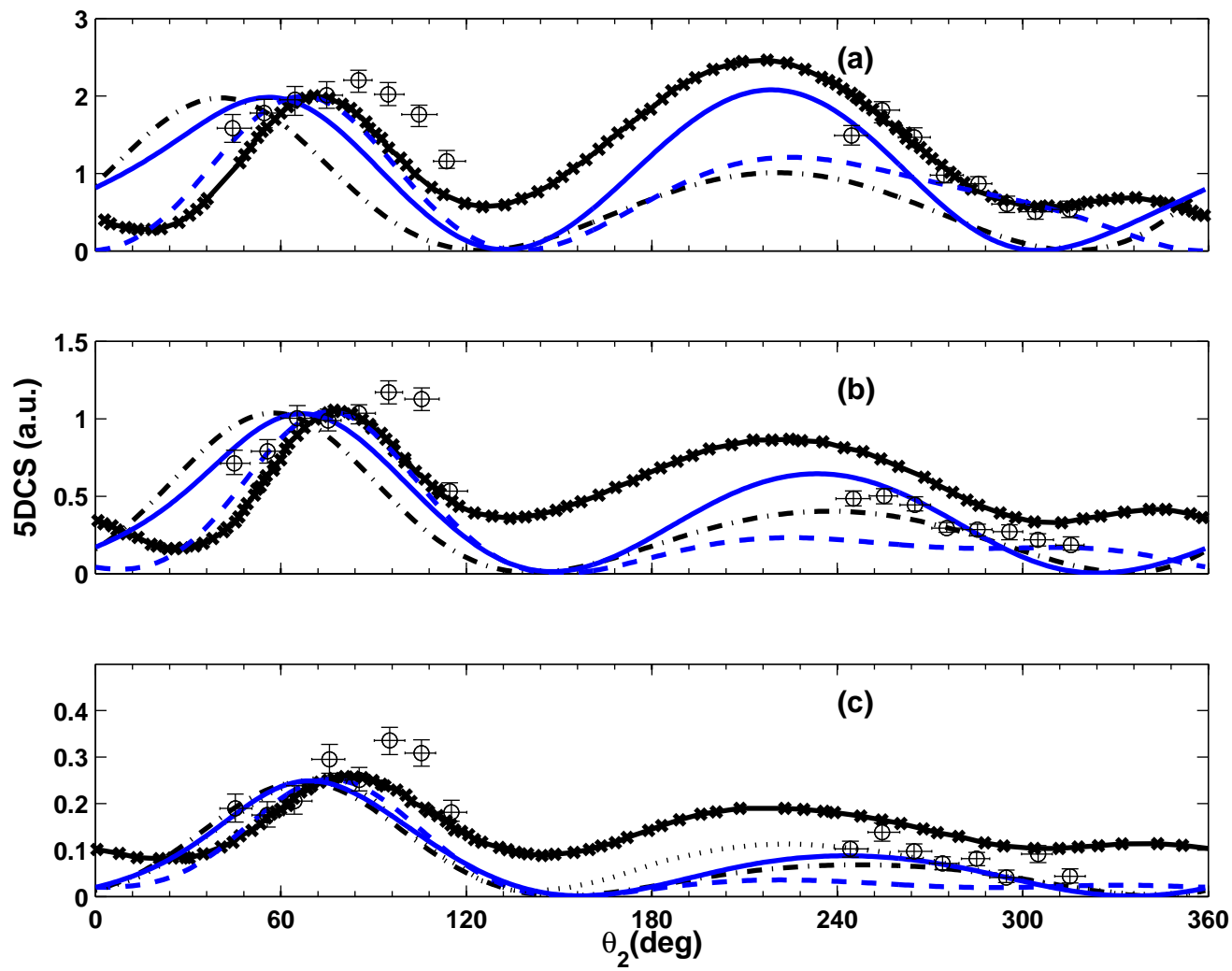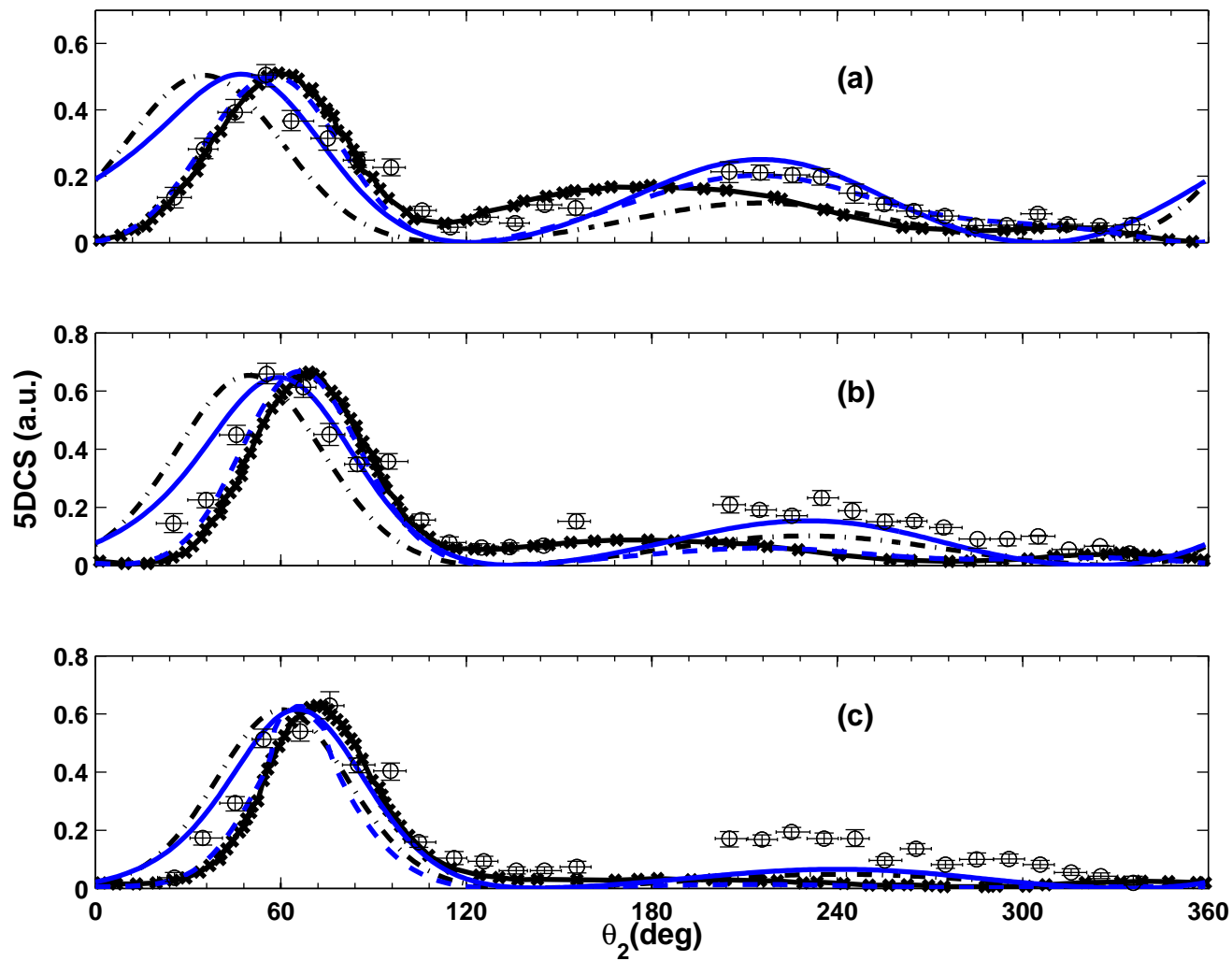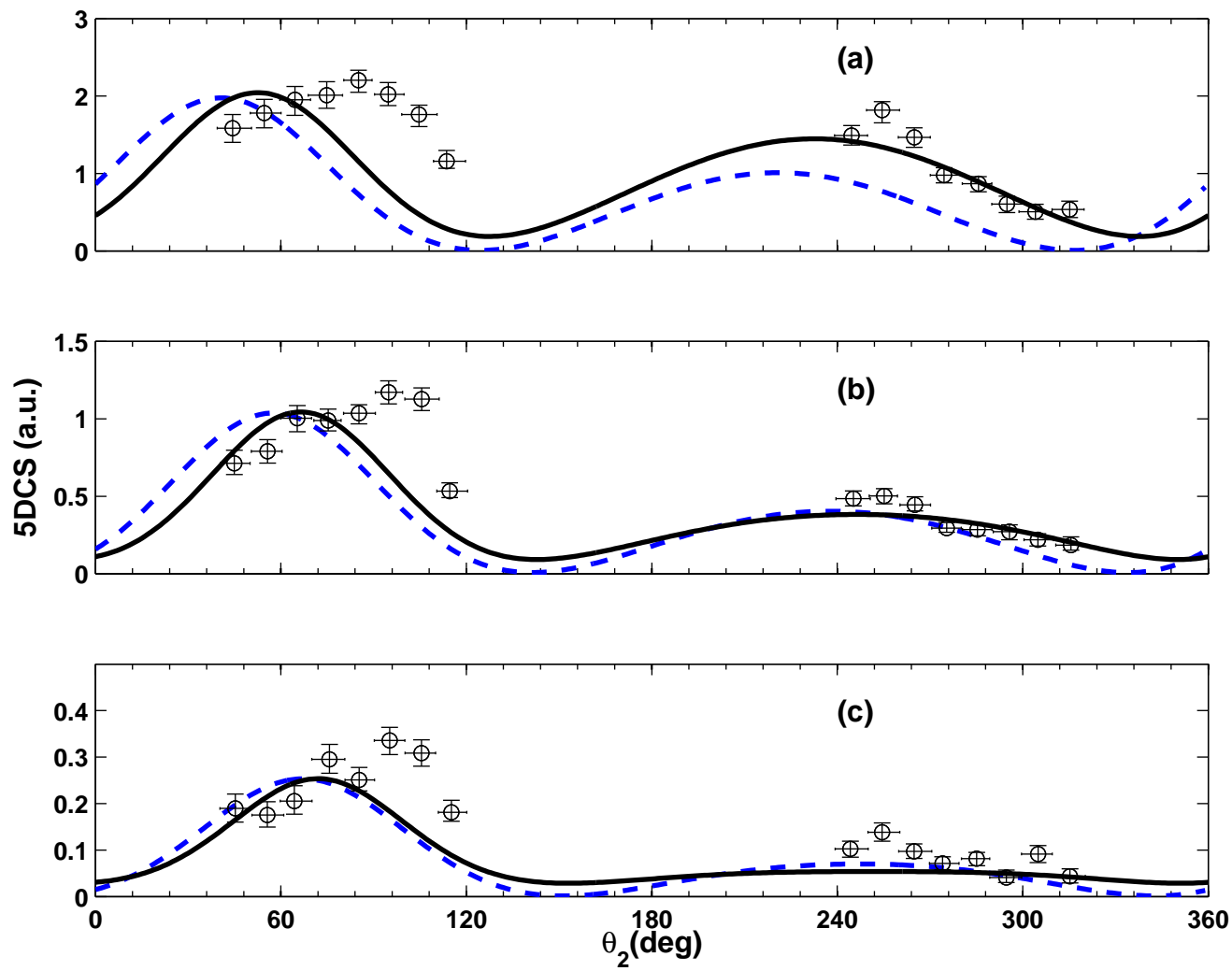
FIG. 1:

18

FIG. 2:

FIG. 3:

FIG. 4:

FIG. 5:

FIG. 6:
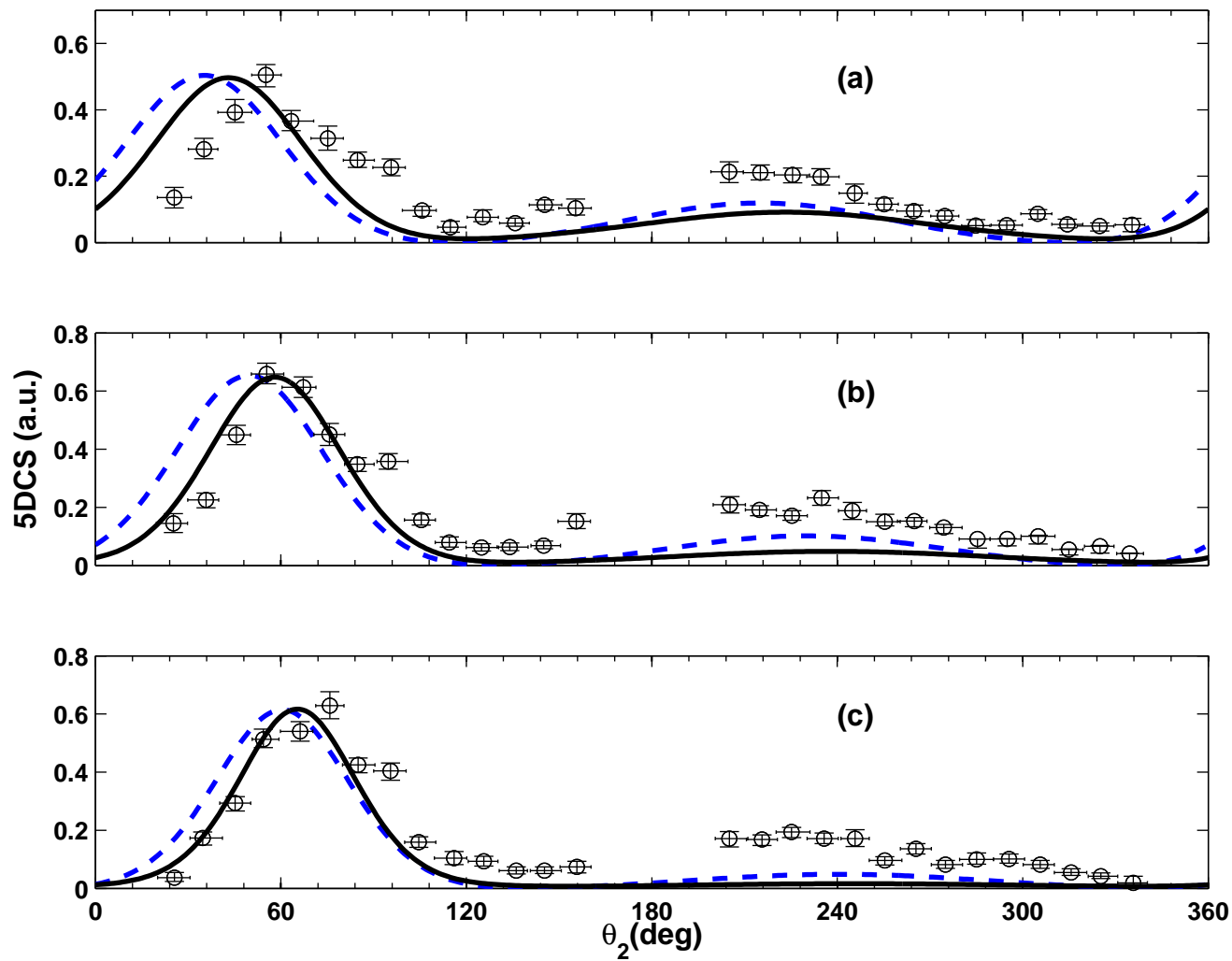
FIG. 7:
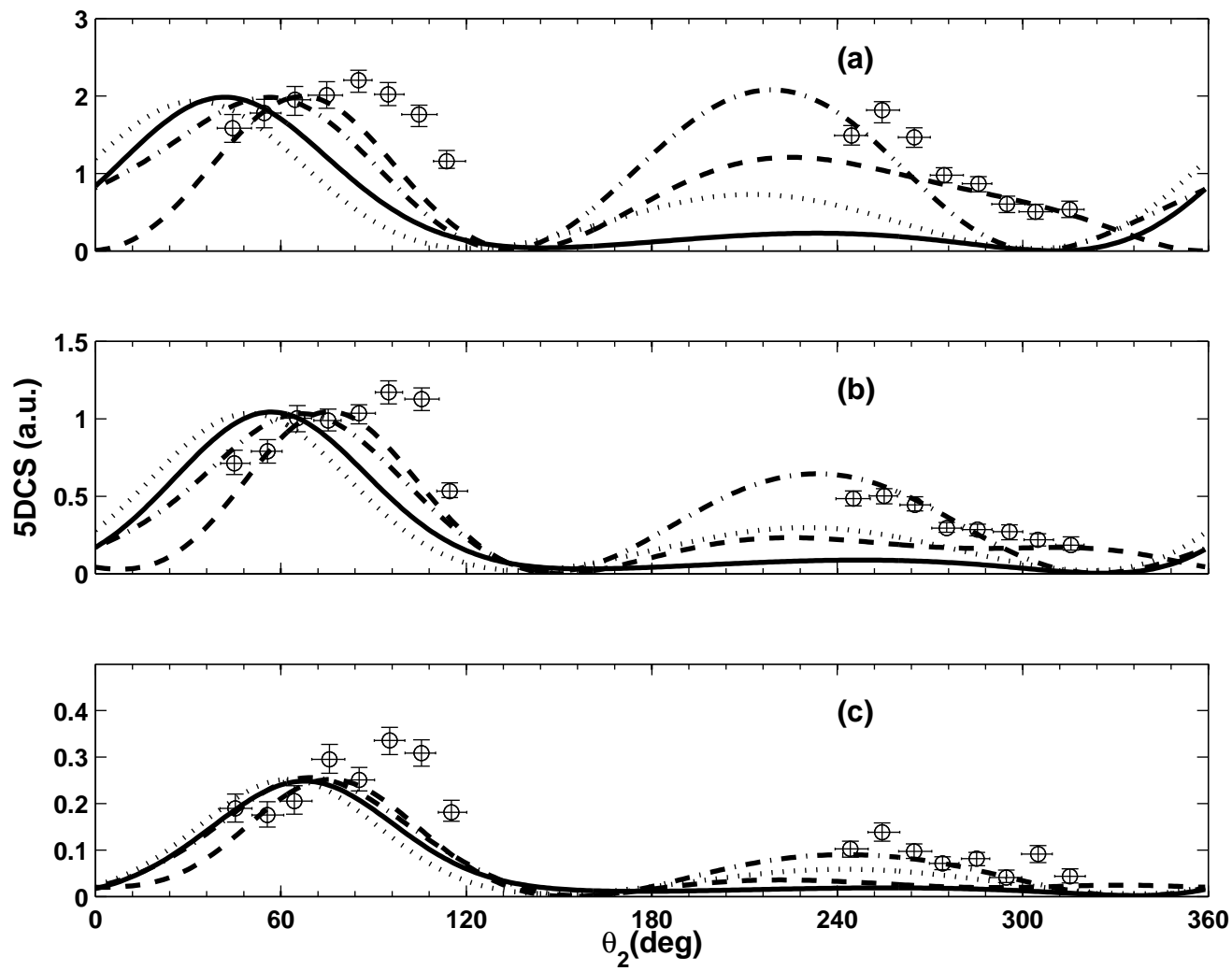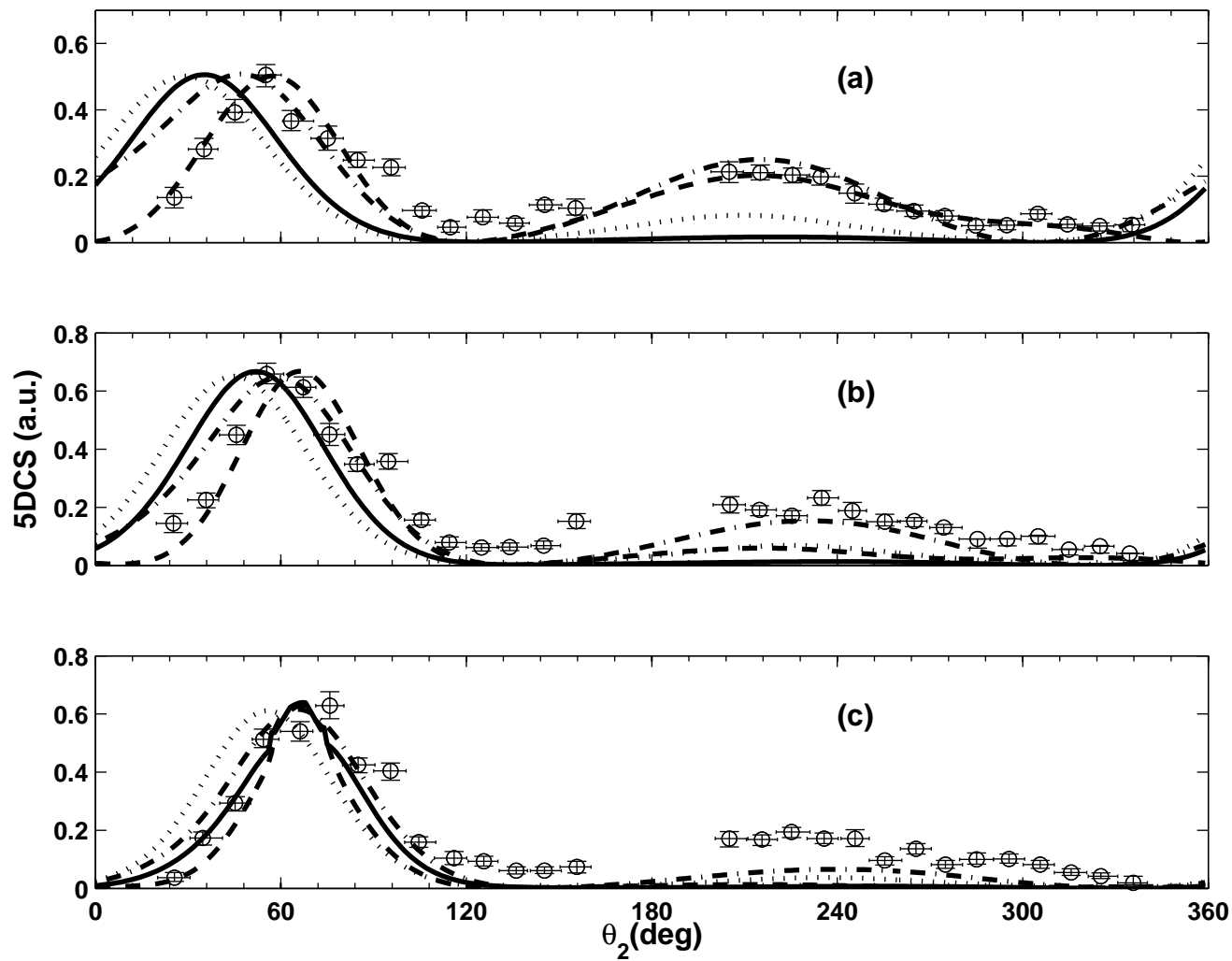
FIG. 8:

FIG. 9:

TABLE 1:

ξ (deg.)	BBK (a.u.)	GA (a.u.)	GA-PCI (a.u.)
E_2=(3.5±2.5) eV and θ_1=(16±4)^o
0	0.448	0.668	0.684
15	0.432	0.643	0.667
30	0.413	0.615	0.647
45	0.397	0.590	0.626
60	0.387	0.576	0.612
75	0.386	0.576	0.608
90	0.395	0.591	0.615

TABLE 2:

θ_1 (deg.)	Peak position	GA (deg.)	GA-PCI (deg.)	BBK (deg.)	3C-He [23] (deg.)	M3DW [28] (deg.)	Expt. [23,28] (deg.)
\multicolumn{8}{c}{E_2=(3.5±2.5) eV and θ_m=90°}
5±2	binary	41.0	56.0	67.0	-	70.0	75.0
	recoil	221.0	219.0	225.0	-	217.0	255.0
9.5±2.5	binary	58.0	67.0	76.0	-	77.0	85.0
	recoil	238.0	234.0	225.0	-	220.0	255.0
16±4	binary	67.0	70.0	76.0	72.0	80.0	75.0
	recoil	247.0	243.0	222.0	222.0	210.0	255.0
\multicolumn{8}{c}{E_2=(16±4.0) eV and θ_m=90°}
5±2	binary	35.0	47.0	57.0	-	60.0	55.0
	recoil	215.0	215.0	214.0	-	180.0	205.0
9.5±2.5	binary	50.0	59.0	66.0	-	69.0	55.0
	recoil	229.0	231.0	216.0	-	178.0	205.0
16±4	binary	60.0	66.0	66.0	-	71.0	75.0
	recoil	240.0	240.0	213.0	-	203.0	205.0

TABLE 3:

E$_2$=(3.5±2.5) eV and θ_m=90°						
θ_1 (deg.)	GA	GA-PCI	BBK	3C-He [23]	M3DW [28]	Expt. [23,28]
5±2	1.957	0.953	1.650	-	0.816	1.106
9.5±2.5	2.571	1.600	4.494	-	1.220	2.060
16±4	3.160	2.830	7.042	2.247	1.363	2.138
E$_2$=(16±4) eV and θ_m=90°						
5±2	4.235	2.026	2.480	-	2.975	2.366
9.5±2.5	6.429	4.210	11.200	-	7.634	3.163
16±4	12.736	9.382	47.093	-	21.348	3.672

TABLE 4:

E$_2$=(3.5±2.5) eV and θ_m=90°				
θ_1 (deg.)	Peak position	GA (deg.)	GA-H (deg.)	Expt. [23,28] (deg.)
5±2	binary	41.0	53.0	75.0
	recoil	221.0	233.0	255.0
9.5±2.5	binary	58.0	66.0	85.0
	recoil	238.0	247.0	255.0
16±4	binary	67.0	72.0	75.0
	recoil	247.0	253.0	255.0
E$_2$=(16±4.0) eV and θ_m=90°				
5±2	binary	35.0	43.0	55.0
	recoil	215.0	223.0	205.0
9.5±2.5	binary	50.0	58.0	55.0
	recoil	229.0	240.0	205.0
16±4	binary	60.0	65.0	75.0
	recoil	240.0	241.0	205.0

TABLE 5:

E$_2$=(3.5±2.5) eV and θ_m=90°			
θ_1 (deg.)	GA	GA-H	Expt. [23,28]
5±2	1.957	1.411	1.106
9.5±2.5	2.571	2.729	2.060
16±4	3.160	4.701	2.138
E$_2$=(16±4) eV and θ_m=90°			
5±2	4.235	5.430	2.366
9.5±2.5	6.429	13.366	3.163
16±4	12.736	38.522	3.672

TABLE 6:

E$_2$=(3.5±2.5) eV and θ_m=90°							
θ_1 (deg.)	GA (e$^-$) (deg.)	GA (e$^+$) (deg.)	GA-PCI (e$^-$) (deg.)	GA-PCI (e$^+$) (deg.)	BBK (e$^-$) (deg.)	BBK (e$^+$) (deg.)	Expt. [23,28] (e$^-$) (deg.)
5±2	41.0	41.0	56.0	32.0	67.0	42.0	75.0
9.5±2.5	58.0	58.0	67.0	50.0	76.0	57.0	85.0
16±4	67.0	67.0	70.0	62.0	76.0	68.0	75.0
E$_2$=(16±4) eV and θ_m=90°							
5±2	35.0	35.0	47.0	29.0	57.0	35.0	55.0
9.5±2.5	50.0	50.0	59.0	45.0	66.0	52.0	55.0
16±4	60.0	60.0	66.0	56.0	66.0	66.0	75.0